

Effect of Elements Connection Types on Mixing Performance of Kenics Static Mixer

Zhijun LI*, Jiankang WANG**, Yiwen ZHENG***, Chenyang WANG****

*School of Mechanical Engineering, Tianjin University of Science and Technology, Tianjin 300222, China,
E-mail: lizj1224@163.com

**Tianjin Key Laboratory of Integrated Design and On-line Monitoring for Light Industry & Food Machinery and Equipment, Tianjin International Joint Research and Development Center of Low-carbon Green Process Equipment, College of Mechanical Engineering, Tianjin University of Science and Technology, Tianjin 300222, China,
E-mail: wangjk@tust.edu.cn (Corresponding author)

***Tianjin Key Laboratory of Integrated Design and On-line Monitoring for Light Industry & Food Machinery and Equipment, Tianjin International Joint Research and Development Center of Low-carbon Green Process Equipment, School of Mechanical Engineering, Tianjin University of Science and Technology, Tianjin 300222, China,
E-mail: 503631057@qq.com

****School of Mechanical Engineering, Tianjin University of Science and Technology, Tianjin 300222, China,
E-mail: wcytust@163.com

<https://doi.org/10.5755/j02.mech.36862>

1. Introduction

Static mixers are widely used in various mixing processes due to their low energy consumption, high efficiency, small size, and low cost [1-4]. Due to without moving parts, their mixing performance more strongly depended on their structures, compare to other mixers. So, study on the relationship between its performance and structure has become a major task in the field. Xingren Jiang et al. [5, 6] studied the effects of mixing element thickness and aspect ratio on performance of Kenics static mixer. The results showed that the thinner the thickness, the lower the pressure drop. In addition, they found that the pressure drop increased with the increase of aspect ratio. Matthew Hildner et al. [7] designed a novel spiral impeller static mixer (Impeller SSM). Though verification they found that the pressure drop of the impeller SSM was 18.2% lower than that of the standard Kenics static mixer. Saied Moghaddam et al. [8] proposed three modified static mixers, and compared their mixing performance with the standard SMX static mixer. The results indicated that the modified static mixer with four blades arranged in 135° cross arrangement had a better mixing performance while pressure drop was consistent. Panggabean et al. [9] simulated the production of biodiesel in a Kenics static mixer with holes using CFD methods. The results showed that the mixing efficiency of the porous spiral mixer was better than that of the traditional spiral mixer. A. Talhaoui et al. [10] designed a new static mixer with helical overlapping mixing elements, and studied the laminar flow and mixing behavior of incompressible Newtonian using CFD simulations, with Reynolds number (Re) from 0.15 to 100. Their research results indicated that compared to the Kenics static mixer, the new static mixer with improved internal geometry had faster mixing speed and better mixing quality. In addition, Sudhanshu S. Soman [11], Vipin Michael [12], Amin Shahbazi [13], Sinthuran Jegatheeswaran [14] and Shiping Liu [15] also studied the mixing effect and pressure drop by changing the structure of static mixer elements.

Besides the element thickness and aspect ratio, the connection type between elements is also an important parameter of Kenics static mixer. However, the literature about it is not almost found. Therefore, the connection types and their sizes are selected in this article, to study their effects on the mixing performance of Kenics static mixer.

2. Methodology

2.1. Geometry

Due to different processing methods, the element connection types of Kenics static mixer are usually divided into four types, including direct jointing, transition blade, plug-in and solder joints. The corresponding static mixers with four types connection are defined as DSM, TSM, PSM and SSM in this work, respectively. DSM and TSM are processed wholly. The former is connected directly without any excess entity between elements. The latter is connected using a small transition blade between elements. PSM and SSM are processed separately with a blade as the element. Their elements are connected using the groove and solder, respectively.

As shown in Fig. 1 and Table 1, the elements of four static mixers have the same exterior dimensions. The

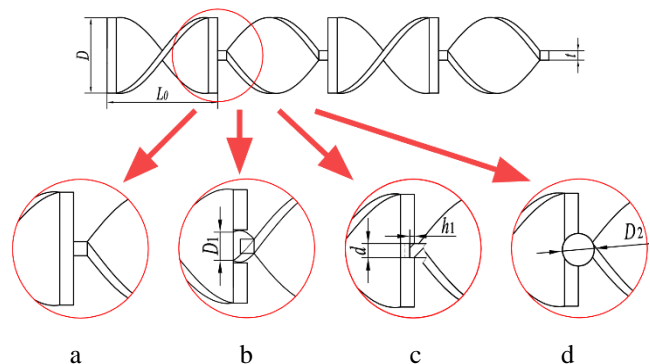


Fig. 1 Four types of static mixers with different connection: a – DSM, b – TSM, c – PSM, d – SSM

diameter (D) is 12 mm, the length (L_0) is 18 mm, the aspect ratio is 1.5 and the thickness (t) is 1.5 mm. Besides that, TSM has a small transition blade with a diameter (D_1) of 3-8 mm, torsion angle 90° and aspect ratio of 0.75. The PSM has a groove with a depth (h_1) of 0.5-2.5 mm and a width (d) of 1.5-3.5 mm. The SSM has a spherical solder joint with a diameter (D_2) of 2-6 mm.

Based on the parameter, the models of static mixers and fluid in them are established using SolidWorks 2020, as shown in Fig. 2.

Table 1

The parameters of static mixers

	Types	D_1 , mm	h_1 , mm	d , mm	D_2 , mm
1	DSM	-	-	-	-
2	TSM3	3	-	-	-
3	TSM4	4	-	-	-
4	TSM5	5	-	-	-
5	TSM6	6	-	-	-
6	TSM7	7	-	-	-
7	TSM8	8	-	-	-
8	PSM0.5	-	0.5	1.5	-
9	PSM1.5	-	1.5	2.5	-
10	PSM2.5	-	2.5	3.5	-
11	SSM2	-	-	-	2
12	SSM3	-	-	-	3
13	SSM4	-	-	-	4
14	SSM5	-	-	-	5
15	SSM6	-	-	-	6

2.2. Problem and basic assumption

Low-Density Polyethylene (LDPE) is employed as the working fluid, acting as both primary and secondary fluids to avoid disturbing the flow pattern by using fluids of different properties [16]. Specific rheological parameters of LDPE are shown in Table 2. The rheology property is expressed using Carreau Yasuda model (shown in Eq. (1)).

$$\eta(\dot{\gamma}) = \eta_\infty + (\eta_0 - \eta_\infty) \left[1 + (\dot{\gamma}\lambda)^a \right]^{(n-1)/a}, \quad (1)$$

where: η_0 is the zero-shear viscosity, λ is the relaxation time, n is the power law exponent, $\dot{\gamma}$ is the shear rate and a is the Yasuda index.

Table 2

The rheology parameters of LDPE

Rheology parameters	η_∞ , Pa·s	η_0 , Pa·s	λ , s ⁻¹	a	n
LDPE	0	11027	0.167	0.362	0.233

The following assumptions are made for the flow of LDPE fluid in the static mixers during simulation [17]:

1. The fluid is an incompressible non-Newtonian fluid.
2. The flow of the fluid is laminar, ignoring inertial forces and gravity.
3. The fluid fills the entire flow channel without any gap.
4. The fluid flows fully in the channel, ignoring the entrance effect.

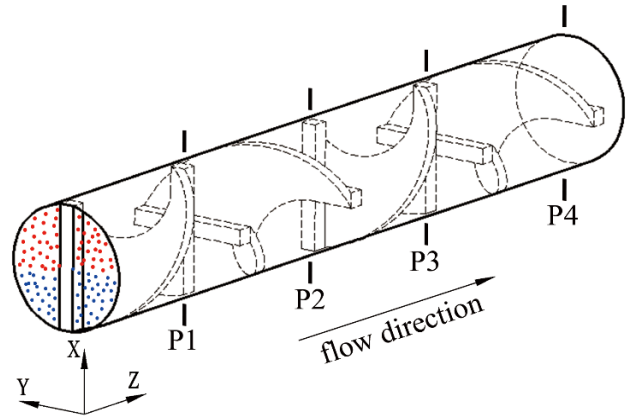


Fig. 2 The distribution of tracer particles on inlet

2.3. Mesh

As shown Fig. 3, all the models are divided into unstructured tetrahedral meshes with the same node density in the X, Y and Z directions, using Workbench 19.1 software.

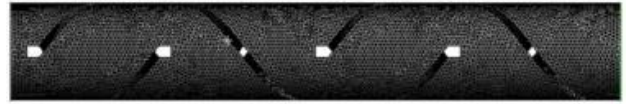
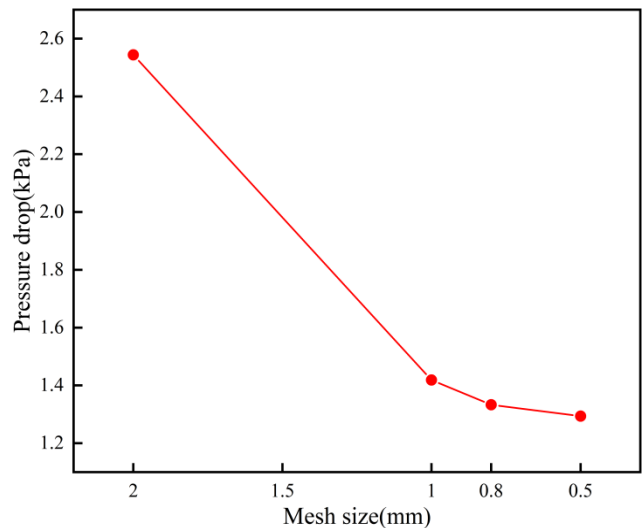


Fig. 3 Schematic diagram of computational domain with meshes

In order to achieve a relatively accurate results while consuming the least time, the mesh independence is carried out with four mesh sizes of 2, 1, 0.8 and 0.5 mm, in which the change of pressure drop (Δp) is selected as an evaluating indicator. As shown in Fig. 4, Δp changes by about 45% while varying mesh size from 2 to 1 mm, however its change is smaller than 2% while varying grid size from 0.8 to 0.5 mm. It is indicated that when the mesh size is smaller than 0.8 mm, the effect of mesh size on the simulation precision can be neglected. Therefore, the mesh size of 0.5 mm is selected to mesh all the models. Using the size, the number of meshes is approximately equal to 500000 in each meshed model.

Fig. 4 The changes of Δp while varying mesh size

2.4. Boundary conditions and calculation method

The boundary conditions are set as follows. The flow rate of 30 ML/min and the pressure of 0.1 MPa are set as the inlet and outlet conditions, respectively. Moreover, no slip is set as the wall condition.

The Picard interpolation method is used to calculate the fluid viscosity, and the implicit Euler method is used to solve the equation, with convergence accuracy of 10^{-5} [18].

2.5. Result characterization

Δp is the pressure loss from inlet to outlet, which is calculated using Eq. (2)

$$\Delta p = p_i - p_o, \quad (2)$$

where p_i and p_o is the average pressure at the inlet and outlet positions, respectively.

There are various characterization indices used to evaluate distribution and mixing in the literature. They include the index of dispersion [19], the aerial distribution [20], the mixing index [21], the coefficient of variation [22] and the segregation scale (S) [23]. In the current study, the S is used to characterize the distribution and mixing of fluid, which is calculated using Eq. (3) and (4).

$$S = \int_0^{\xi} (R|r|) d|r|, \quad (3)$$

$$R|r| = \frac{\sum_{i=1}^M (C_i' - \bar{C})(C_i'' - \bar{C})}{M\sigma^2}, \quad (4)$$

where: $R|r|$ is the Euler correlation coefficient between the pairing particles concentrations separated by distance $|r|$. Specifically, $R(0) = 0$ indicates that the pairing particles have similar correlations, and $R(\xi) = 1$ indicates that the pairing particles have no correlation. σ^2 is the sample variance. M is the number of pairing particles. C_i' and C_i'' are the concentrations of the i -th pairing particles, while \bar{C} represents the average concentration.

In addition, 3000 tracer particles with red and blue colors flow into the channel of the static mixers, from two sides of the entrance, respectively. Four planes P1, P2, P3 and P4 perpendicular to the flow direction are selected to observe the distributions of tracer particles, as shown in Fig. 2.

3. Result and Discussion

3.1. Velocity and streamline

As shown in Fig. 5, the fluid flow through each static mixer in a spiral form. When the connection size is small, such as TSM3, PSM0.5 and SSM3, their velocity streamlines are similar to the DSM's. However, as the connection size is larger, such as TSM8, PSM2.5 and SSM6, the effects of connection types on streamline is significant. The larger velocity appears near the connection of TSM, PSM and SSM, compare to DSM. It is because that the flow space is reduced due to the connection size increasing, which results in that the speed of fluid increases when the

flow rate is constant. Moreover, it is found that the effect of connection size on the velocity is larger in PSM, than that in TSM and SSM. It maybe because that the overlap between two adjacent blades with opposite rotation directions makes flow transition from a spiral form to a straight form in PSM. This influence is larger than the local changing flow direction in TSM, and only reducing flow cross-section in SSM.

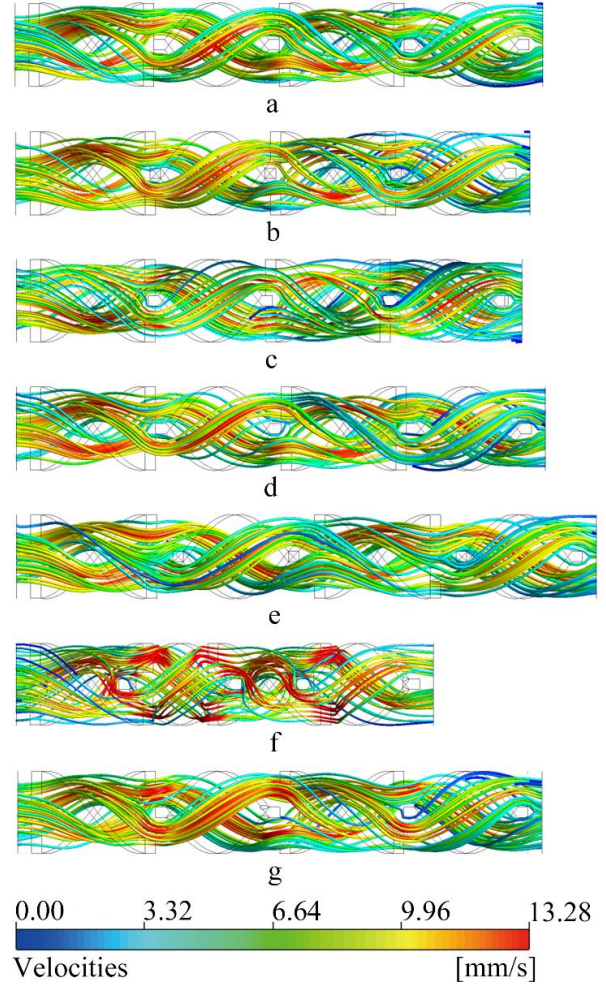


Fig. 5 The streamline of fluid in the static mixers: a - DSM, b - TSM3, c - PSM0.5, d - SSM3, e - TSM8, f - PSM2.5, g - SSM6

3.2. Pressure drop

The pressure decreases approximately linearly with the flow in all static mixers. However, Δp is different in them. It increases with connection size increasing in TSM, PSM and SSM, and almost all are larger than Δp of in DSM, which is 1.29 MPa.

In TSM, the change of Δp is small as varying connection size from 3 to 8 mm, which is only 4.7%. The Δp of all TSM are near to that of DSM, as shown in Fig. 6-a. However, it is found in Fig. 6, b that the change of Δp in PSM is large as varying connection size from 0.5 to 2.5 mm, which is 96.3%. Compared to DSM, the Δp of PSM0.5, PSM1.5 and PSM2.5 increase by 3.9%, 24.0% and 103.9%, respectively. The similar trends are seen in Fig. 6, c. The Δp of SSM is increased from 1.29 to 1.48 MPa while varying connection size from 2 to 6 mm. The largest one in SSM is 14.7% larger than that in DSM. The more detailed data about Δp are showed in Table 3.

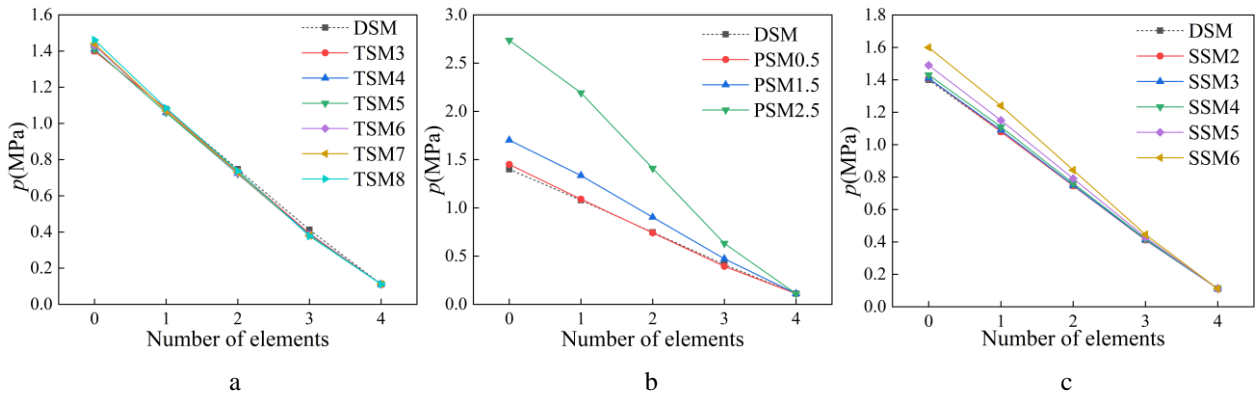


Fig. 6 Pressure variation of a – TSM, b – PSM, c – SSM

Table 3

The Δp of static mixers

Static mixer \ Δp , MPa	Connection size, mm										
	0	0.5	1.5	2	2.5	3	4	5	6	7	8
DSM	1.29	-	-	-	-	-	-	-	-	-	-
TSM	-	-	-	-	-	1.29	1.29	1.30	1.32	1.33	1.35
PSM	-	1.34	1.60	-	2.63	-	-	-	-	-	-
SSM	-	-	-	1.29	-	1.29	1.32	1.38	1.48	-	-

From the above data, it can be concluded that the effect of connection size of PSM on the Δp is the largest in three static mixers, then SSM, the last one is TSM. It is consistent with the results shown in Fig. 6.

3.3. Segregation scale

The S shows a decreasing trend overall with the flow in the static mixers. In addition, when the connection size is small, the S of TSM, PSM and SSM are near to or even smaller than the one of DSM, such as in TSM3, PSM0.5 and SSM2. Nevertheless, when the connection size is large, the S of TSM, PSM and SSM are obviously larger

than the one of DSM. For example, the S of TSM8 is 600.5% larger, the S of PSM2.5 is 191.3% larger, and the S of SSM6 is 35.7% larger than the one of DSM. The more detailed data about S can be found in Fig. 7, a, b and c.

Similar to the effect of connection size on velocity stream and Δp , there are the largest effect of connection size on S in the PSM. In all static mixers, the smallest and largest S are found in PSM0.5 and TSM8, respectively. They are 0.101 and 0.667 mm, which have 13.9% and 600.5% changes relative to the S of DSM. In addition, the SSM has a smaller effect of connection size on S than TSM, although it has a larger effect on Δp than the latter.

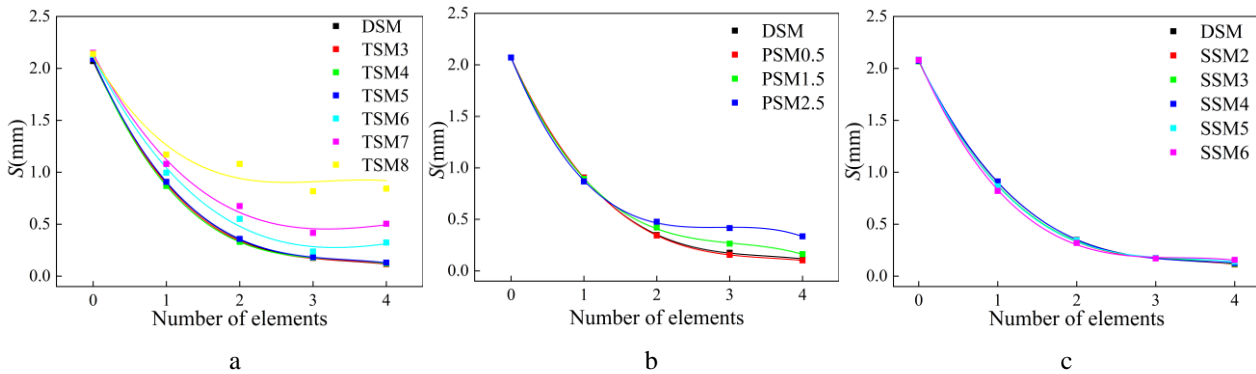


Fig. 7 Segregation scale of a – TSM, b – PSM, c – SSM

3.4. Distribution of tracer particles

The particle distribution diagram of DSM and TSM3, as shown in Fig. 8, a and b, is similar to PSM0.5 and SSM3. It can be seen that the distributions of tracer particles are similar in four types of static mixers, when the connection size is small. The tracer particles are gradually mixed in laminate form. From P1 to P4, the number of red and blue particles alternating layer increases and the thickness of layer declines uniformly.

This neglected difference of particles distributions is same with that of velocity stream and Δp , when the connection size is small.

As shown in Fig. 9, when the connection size is large, the significant difference appears among them. The obvious agglomeration of particles is observed in TSM and PSM, such as TSM8 and PSM2.5. But the phenomenon is not found in SSM, even in SSM6. It is again demonstrated that the effect of connection size on the mixing performance is little in SSM.

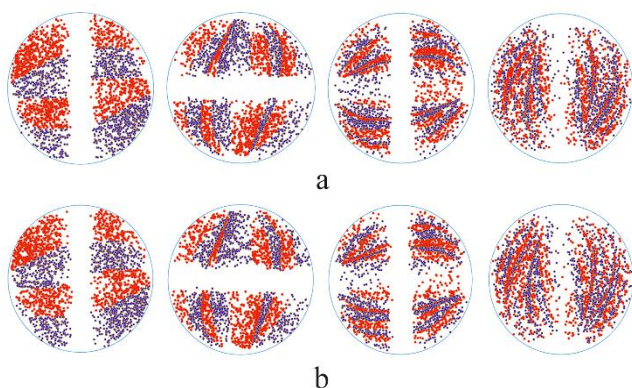


Fig. 8 Radial slice particle distribution: a – DSM, b – TSM3

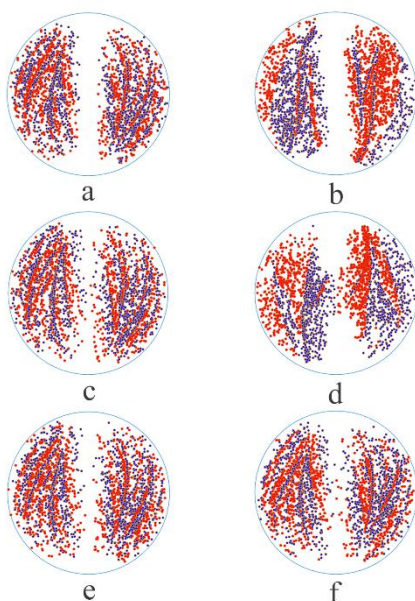


Fig. 9 The distribution of tracer particles on P4: a – TSM3, b – TSM8, c – PSM0.5, d – PSM2.5, e – SSM3, f – SSM6

4. Conclusion

Four types of Kenics static mixers with different connection forms, including direct jointing type (DSM), transition blade type (TSM), plug-in type (PSM) and solder joint type (SSM) are selected to study the effects of connection type and size on the mixing performance through simulation. The velocity stream line, pressure drop (Δp), segregation scale (S) and distribution of tracer particles are investigated famously, the specific conclusions are as follows:

1. In general, as the flow progresses, the Δp decreases approximately linearly, and the S decreases nonlinearly. In addition, the speed, Δp and S augment while increasing connection size in TSM, PSM and SSM. And the phenomenon of agglomeration among particles becomes obvious in TSM and PSM, but the phenomenon is not found in SSM. A better mixing performance is found in DSM or the other three static mixers with a small connection size. The smallest Δp of 1.29 MPa are found in DSM, TSM3 and SSM2. The smallest S of 0.101 mm are found in PSM0.5.

2. When the connection size is small, the mixing performance of TSM, PSM and SSM are similar to that of DSM. However, when the connection size is large, there are

a significant difference between them. Especially, PSM has the largest effect of connection size in all static mixers.

3. The largest Δp and S of TSM are 4.7% and 600.5% larger than those of DSM. Those of PSM are 103.9% and 191.3% larger than those of DSM. And those of SSM are 14.7% and 35.7% larger than those of DSM.

Acknowledgement

This work is supported by Tianjin DTH Mixer Machinery Co., Ltd.

References

- Li, Y. D.; Wu, S. H.; Liu, Y. Q.; Wang, N.; Dai, P. Y.; Yang, Q.; Lu, H. 2022. The coupled mixing action of the jet mixer and swirl mixer: A novel static micromixer, *Chemical Engineering Research and Design* 177: 283-290. <https://doi.org/10.1016/j.cherd.2021.10.040>.
- Pezo, L.; Pezo, M.; Jovanović, A.; Čolović, R.; Vukmirović, D.; Banjac, V.; Đuragić, O. 2018. The joint mixing action of the static pre-mixer and the rotating drum mixer-Discrete element method approach, *Advanced Powder Technology* 29(7):1734-1741. <https://doi.org/10.1016/j.apt.2018.04.008>.
- Albertazzi, J.; Florit, F.; Busini, V.; Rota, R. 2021. Mixing Efficiency and Residence Time Distributions of a Side-Injection Tubular Reactor Equipped with Static Mixers, *Industrial & Engineering Chemistry Research* 60(29): 10595-10602. <https://doi.org/10.1021/acs.iecr.1c00575>.
- Santana, S. H.; Tortola, S. D.; Silva, J. L.; Taranto, O. P. 2017. Biodiesel synthesis in micromixer with static elements, *Energy Conversion and Management* 141: 28-39. <http://doi.org/10.1016/j.enconman.2016.03.089>.
- Jiang, X. R.; Xiao, Z. D.; Jiang, J. N.; Yang, X. X.; Wang, R. J. 2021. Effect of element thickness on the pressure drop in the Kenics static mixer, *Chemical Engineering Journal* 424: 130399. <https://doi.org/10.1016/j.cej.2021.130399>.
- Jiang, X. R.; Yang, N.; Wang, R. J. 2021. Effect of Aspect Ratio on the Mixing Performance in the Kenics Static Mixer, *Processes* 9(3): 464. <https://doi.org/10.3390/pr9030464>.
- Hildner, M.; Lorenz, J.; Zhu, B. Z.; Shih, A. 2023. Pressure drop reduction of the impeller spiral static mixer design enabled by additive manufacturing, *Chemical Engineering and Processing-Process Intensification* 191: 109486. <https://doi.org/10.1016/j.cep.2023.109486>.
- Moghaddam, S. 2023. Effect of Non-Newtonian Fluid on Mixing Quality and Pressure Drop in Several Static Mixers: A Numerical Study, *Iranian Journal of Science and Technology, Transactions of Mechanical Engineering* 47:1585-1597. <https://doi.org/10.1007/s40997-023-00621-5>.
- Panggabean, S.; Sigalingging, R.; Raju. 2020. Simulation of biodiesel production using perforated helical type static mixer, *IOP Conference Series Earth and Environmental Science* 454(1): 012045. <https://doi.org/10.1088/1755-1315/454/1/012045>.

10. **Talhaoui, A.; Draoui, B.; Youcefi, A.** 2020. Effect of Geometry Design on Mixing Performance of Newtonian Fluids using Helical Overlapped Mixer Elements in Kenics Static Mixer, *Journal of Applied Fluid Mechanics* 14(6):1643-1656.
<https://doi.org/10.47176/jafm.14.06.32494>.
11. **Soman, S. S.; Madhuranthakam, C. M. R.** 2017. Effects of internal geometry modifications on the dispersive and distributive mixing in static mixers, *Chemical Engineering and Processing: Process Intensification* 122: 31-43.
<http://doi.org/10.1016/j.cep.2017.10.001>.
12. **Michael, V.; Dawson, M.; Prosser, R.; Kowalski, A.** 2022. Laminar flow and pressure drop of complex fluids in a Sulzer SMX+™ static mixer, *Chemical Engineering Research and Design* 182: 157-171.
<https://doi.org/10.1016/j.cherd.2022.03.018>.
13. **Shahbazi, A.; Ashtiani, H. A. D.; Afshar, H.; Jafarkazemi, F.** 2021. Optimization of the SMX static mixer types thermal and hydraulic performance by coupling CFD-Genetic Algorithm, *International Communications in Heat and Mass Transfer* 126:105388.
<https://doi.org/10.1016/j.icheatmasstransfer.2021.105388>.
14. **Jegatheeswaran, S.; Ein-Mozaffari, F.; Wu, J. N.** 2017. Process intensification in a chaotic SMX static mixer to achieve an energy-efficient mixing operation of non-newtonian fluids, *Chemical Engineering and Processing: Process Intensification* 124: 1-10.
<https://doi.org/10.1016/j.cep.2017.11.018>.
15. **Liu, S. P.; Hrymak, A. N.; Wood, P. E.** 2005. Design modifications to SMX static mixer for improving mixing, *AIChE Journal* 52(1): 150-157.
<https://dx.doi.org/10.1002/aic.10608>.
16. Ansys (2019). POLYFLOW 19.1 User's Guide.
17. **Sun, J. G.; Wang, J. K.; Zheng, Y. W.; Li, Z. J.** 2023. Tuning of Mixing Zone Parameters in a Dynamic Mixer and Performance Comparison with Screw-Based Mixer, *Mechanika* 29(4): 309-316.
<https://doi.org/10.5755/j02.mech.33213>.
18. **Belhout, C.; Bouzit, M.; Menacer, B.; Kamla, Y.; Ameer, H.** 2020. Numerical Study of Viscous Fluid Flows in a Kenics Static Mixer, *Mechanika* 26(3): 206-211.
<http://dx.doi.org/10.5755/j01.mech.26.3.24160>.
19. **Kukukova, A.; Aubin, J.; Kresta, S. M.** 2009. A new definition of mixing and segregation: Three dimensions of a key process variable, *Chemical Engineering Research and Design* 87(4): 633-647.
<https://doi.org/10.1016/j.cherd.2009.01.001>.
20. **Forte, G.; Albano, A.; Simmons, M. J. H.; Stitt, H. E.; Brunazzi, E.; Alberini, F.** 2019. Assessing Blending of Non-Newtonian Fluids in Static Mixers by Planar Laser Induced Fluorescence and Electrical Resistance Tomography, *Chemical Engineering & Technology* 42(8): 1602-1610.
<https://doi.org/10.1002/ceat.201800728>.
21. **Nadeem, H.; Subramaniam, S.; Nere, N. K.; Heindel, T. J.** 2023. A particle scale mixing measurement method using a generalized nearest neighbor mixing index, *Advanced Powder Technology* 34(2): 103933.
<https://doi.org/10.1016/j.apt.2022.103933>.
22. **Chakleh, R.; Azizi, F.** 2023. Performance comparison between novel and commercial static mixers under turbulent conditions, *Chemical Engineering and Processing - Process Intensification* 193: 109559.
<https://doi.org/10.1016/j.cep.2023.109559>.
23. **Zheng, Y. W.; Wang, J. K.; Sun, J. G.; Wang, C. Y.** 2023. Design and Optimization of Online Dynamic Mixer and Its Performance Analysis, *Journal of Applied Fluid Mechanics* 16(9): 1742-1751.
<https://doi.org/10.47176/JAFM.16.09.1752>.

Z. Li, J. Wang, Y. Zheng, C. Wang

EFFECT OF ELEMENTS CONNECTION TYPES ON MIXING PERFORMANCE OF KENICS STATIC MIXER

S u m m a r y

In this work, we analyzed the influence of four connection types of Kenics static mixer, namely direct connection static mixer (DSM), transition blade static mixer (TSM), plug-in static mixer (PSM) and solder joints static mixer (SSM) on the mixing performance. The effects of transition blade diameter, groove depth and solder joint diameter on segregation scale (S) and pressure drop (Δp) were studied. The results indicated that a better mixing performance and Δp were found in the mixers of DSM and three other small-sized connection types. The smallest Δp of 1.29 MPa were found in DSM, TSM3 and SSM2. The smallest S of 0.101 mm were found in PSM0.5. In addition, Δp and S increased as the connection size increases, in TSM, PSM and SSM. The agglomeration of particles was obvious in TSM and PSM with large connection sizes, but not in SSM.

Keywords: static mixer, connection types, numerical simulation, pressure drop, segregation scale.

Received April 2, 2024

Accepted October 22, 2024



This article is an Open Access article distributed under the terms and conditions of the Creative Commons Attribution 4.0 (CC BY 4.0) License (<http://creativecommons.org/licenses/by/4.0/>).